Magnesium Technology 2013
Edited by: Norbert Hort, Suveen N. Mathaudhu, Neale R. Neelameggham, and Martyn Alderman
TMS (The Minerals, Metals & Materials Society), 2013

In situ synchrotron diffraction of the solidification of Mg-RE alloys

D. Tolnai, C.L. Mendis, A. Stark, G. Szakács, B. Wiese, K.U. Kainer, N. Hort

Helmholtz-Zentrum Geesthacht, Institute of Materials Research, Max-Planck Str. 1, D – 21502 Geesthacht, Germany

Keywords: Magnesium Rare Earth alloys, Solidification, In situ synchrotron diffraction

Abstract

Mg-RE alloys have a good potential to be used in bio-applications as degradable implants. Their macroscopic characteristics are strongly dependant on the microstructure, which can be tailored through the alloy composition and the solidification parameters. *In situ* synchrotron diffraction provides a unique tool to follow the phase formation, possible meta-stable and stable phase transformations and grain growth during cooling. In the present study Mg alloys containing Gd, Y and Nd were investigated to characterize the solidification phenomenon during cooling from 680°C to room temperature. Samples were melted and solidified in a Bähr 805 dilatometer modified for *in situ* synchrotron measurements. The molten samples were contained in steel crucibles, and the temperature was controlled by type S thermocouples during cooling. The results provide an experimental validation of thermodynamic calculations; and provide experimental input for refining the thermodynamic models, which contribute to the better understanding of the microstructure evolution to control desirable macroscopic characteristics.

Introduction

Based on their promising mechanical and corrosion properties Mg-RE based alloys are attractive for structural [1] and as well for biomaterial applications [2]. Y, Gd and Nd are important alloying elements for these types of materials. Gd has a maximum solubility of 23.49 wt% at 548 °C [3] and offers both solid solution strengthening and precipitation hardening. The Mg_5Gd, phase forms at the grain boundaries during casting of Mg-Gd alloys [3]. These particles have a size in the micrometer range. During solution heat treatment they dissolve until the maximum solubility at the given temperature. A T6 heat treatment leads to the precipitation of fine particles. The selected area diffraction investigations using transmission electron microscopy (TEM) indicate that these fine precipitates are the meta-stable phases β' and β'' after peak hardness at 250°C. The β' phase is homogeneously distributed over the matrix, while β'' is only observed heterogeneously at peak hardness. The β'' phase is isomorphous with Mg and the precipitates are coherent. The lattice parameter of β' is twice that of Mg and has a c-based centred orthorhombic structure (a = 0.641 nm, b = 2.223 nm, c = 0.521 nm) [2].

Nd has a maximum solubility of ~ 3 wt % at 548 °C therefore the main strengthening mechanism is precipitation hardening by the $Mg_{12}Nd$ phase mainly at the grain boundaries. During solution heat treatment they spheroidize, while the T6 treatment leads to the precipitation of the β' Mg_3Nd phase. The β' has a fcc structure with a lattice parameter a ≈ 0.375 nm [4]. Mg-Y-Nd based alloys, such as WE43 and WE54 form an important class of cast magnesium alloys used in elevated temperature applications with superior mechanical properties at both room and elevated temperatures [5]. The WE54 and WE43 alloys are conventionally used in the T6 condition with the precipitation hardening response as well as the sequence and crystal structure of the resultant phases investigated before [6-9]. The intermetallic phases found in the as-cast Mg-5Y-2Nd (wt%) and Mg-4Y-2Nd (wt%) alloys have been characterized, with transmission electron microcopy to be a ternary phase with a face centered cubic crystal structure with a = 2.223 nm and a composition of $Mg_{14}Nd_2Y$ [10] or $Mg_{15}Nd_2Y$ [9].

However, no detailed studies on the microstructural evolution during solidification from the melt has been conducted to date even though majority of these alloys are used as heat treated sand or permanent mould castings and, as such, their microstructure is determined during solidification. The macroscopic mechanical properties of multiphase materials depend strongly on the chemical composition, volume fraction and spatial distribution of the internal phases [11] which are determined during solidification. Additionally, the cast microstructures influence structure-property relationships of the alloys during subsequent thermo-mechanical processing. Therefore the understanding of the sequence of formation and evolution of the internal phases during solidification is a prerequisite to achieve control of the microstructure of these alloys.

The thermodynamic databases and binary phase diagrams [3] provide information on the presumed solidification path. Based on this data, the resultant microstructure can be modeled [12]. The majority of the commercial Mg alloys are not binary, but complex alloys with more, than one alloying addition. For these materials the information in the simulation databases is limited. Thus the simulation of the experimentally observed microstructure and modeling of the solidification sequence is not feasible due to the lack of available data. To investigate solidification phenomenon experimentally, traditionally ex situ measurements were performed. The cooling is interrupted at different temperatures i.e. at different stages of the microstructure development. The quenched samples can be investigated *ex situ* by conventional metallographic methods in order to characterize the phases and to quantify microstructural parameters [13-15]. The advantage of this method is its relative simplicity, while its disadvantage is that it lacks time-temperature resolution of the investigated solidification process. The continuous development of the X-ray acquisition systems at synchrotron sources provides a unique tool to characterize the phase formation and evolution during the solidification *in situ*. Recording the diffraction patterns while cooling the system down, allows to identify the internal phases, to determine their solidification sequence [16,17] and to use these results as experimental validation of the existing thermodynamic databases and in certain cases contribute to the completion of them.

The present study reports results of *in situ* synchrotron diffraction studies conducted during solidification of Mg-RE alloys, and their comparison with the existing thermodynamic data on this system.

Experimental methods

The alloys Mg-15Gd and Mg-4Y-3Nd (wt %) were chosen for the experiments, as they are of particular interest in structural and in biomaterial applications. The microstructures of the alloys were examined with a Carl Zeiss Gemini Ultra 55 scanning electron microscope (SEM) operating at 15kV equipped with an EDAX energy dispersive X-ray spectrometer (EDXS).

For the diffraction experiments small samples taken from the materials in as-cast condition; were encapsulated in steel crucibles. The measurements were carried out at the HZG beamline HARWI II of the Hamburger Synchrotronstrahlungslabor (HASYLAB) at the Deutsches Elektronen-Synchrotron (DESY). The experiments were performed inside the coil of a DIL 805A/D dilatometer (Bähr-Thermoanalyse GmbH, Hüllhorst, Germany). The experimental setup is shown in Figure 1.

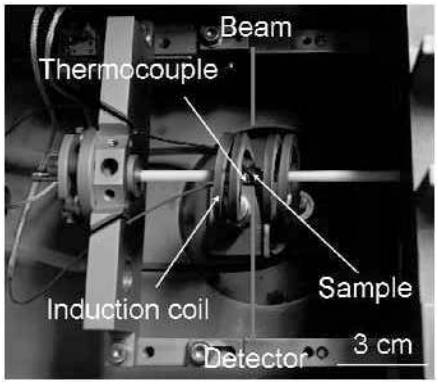

Figure 1. Experimental setup of the *in situ* solidification experiment inside the chamber of a Bähr 805A/D dilatometer modified for *in situ* synchrotron measurements. The windows on the sides are covered by Kapton foil, while the coil is opened, for the beam to pass through the sample.

During the tests the samples were held in sealed stainless steel crucibles in order to hold the molten metal and to isolate it from the surrounding atmosphere. The dilatometer has been modified to meet the requirements of *in situ* synchrotron measurements. The two windows on the sides covered by Kapton foils, prevent interference with the X-ray beam. The windings of the induction coil are opened so the beam only passes through the sample [18]. The temperature was regulated by a type S thermocouple welded on the crucible containing the sample. The heating and cooling was performed in Ar flow.

To melt the samples the system was heated up to 680 °C, held for 5 min was and then cooled to 180 °C at a cooling rate of 5 K/min for the Mg15Gd samples and of 10 K/min for the Mg4Y3Nd samples, respectively.
The *in situ* diffraction experiments were conducted in transmission geometry using a beam with a cross section of 1 × 1 mm^2. In order to penetrate the sample inside the crucibles, high-energy X-rays were used with a photon energy of 100 keV, corresponding to a wavelength of λ = 0.0124 nm. During the experiment the Debye-Scherrer diffraction rings were recorded in every 25 s (~ 2.5 K and ~ 5 K) by a mar555 flatpanel detector (Marresearch GmbH, Norderstedt, Germany) with an area of 3070×2560 pixels with a pixel size of 140 µm². Conventional diffraction patterns (line diagrams) were achieved by filtering the detector image to avoid the effect of hot pixels, followed by an azimuthal integration of the Debye-Scherrer rings.

Results

Microstructure

The secondary electron micrograph of Mg15Gd in as-cast condition is shown in Figure 2.

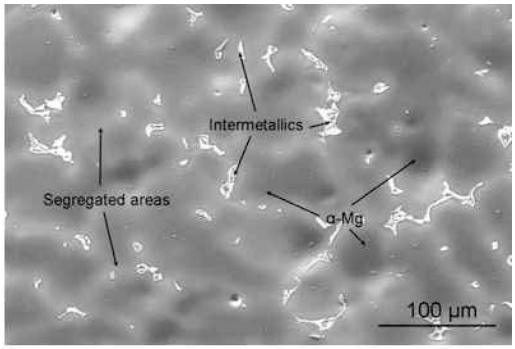

Figure 2 Secondary electron micrograph of the investigated Mg-15Gd alloy in as-cast condition.

The microstructure consists of α-Mg dendrites, segregated regions and intermetallic particles identified as Mg_5Gd using EDXS. The secondary electron micrograph of Mg-4Y-3Nd in as-cast condition is shown in Figure 3.

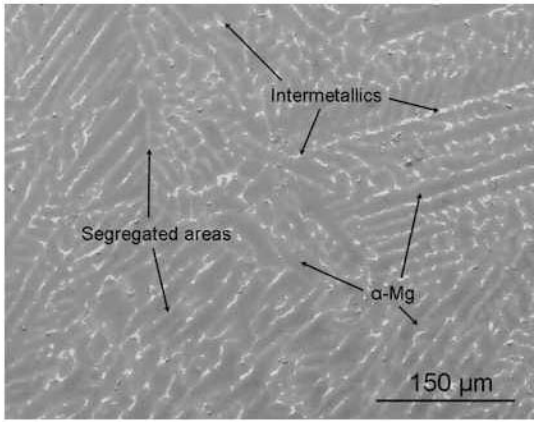

Figure 3 Secondary electron micrograph of the investigated Mg-4Y-3Nd alloy in as-cast condition.

The alloy contains α-Mg dendrites, segregated regions and intermetallic particles with Y and Nd, identified as; $Mg_{24}Y_5$-, $Mg_{12}Nd$-binary phases and a ternary phase $Mg_{14}Y_4Nd$ using EDXS.

In situ synchrotron diffraction

The line profiles resulting from the azimuthal integration of the 2D diffraction patterns acquired during solidification are shown in Figure 4 for Mg15 Gd and in Figure 5 for Mg4Y3Nd, respectively.

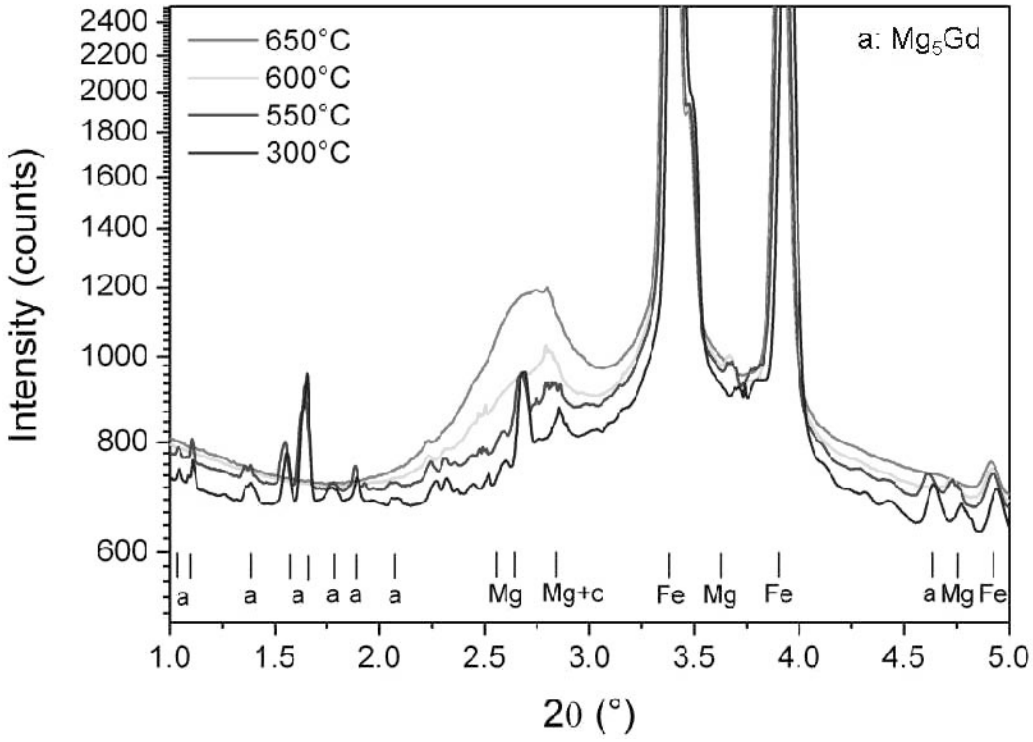

Figure 4 Sequence of XRD line diagrams obtained by the integration of the diffraction patterns recorded during solidification of Mg15Gd. (Wavelength λ = 0.0124 nm)

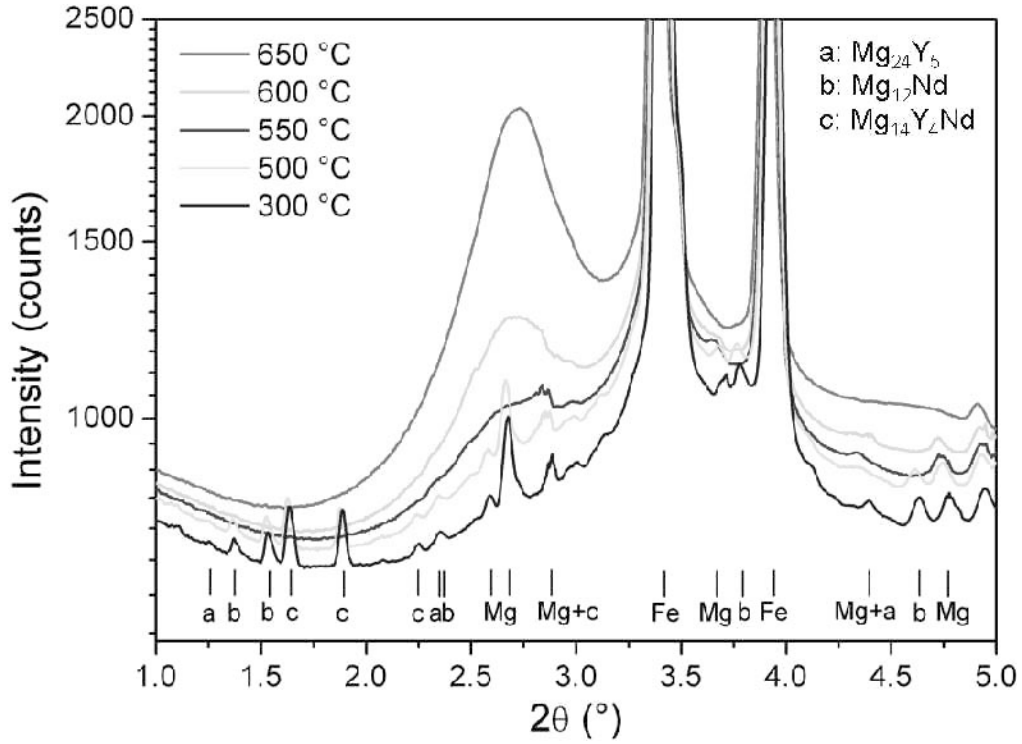

Figure 5 Sequence of XRD line diagrams obtained by the integration of the diffraction patterns recorded during solidification of Mg4Y3Nd. (Wavelength λ = 0.0124 nm)

From indexing the peaks in the line profiles the solidification sequence of the alloys can be determined with a temperature resolution of ~ 3 °C (5 °C in the case of Mg-4Y-3Nd). When the samples are molten only a diffuse background originating from the melt and the peaks of the steel crucibles are observed. In case of the Mg-15Gd (Figure 4) the solidification starts with the α-Mg grains at a measured temperature of 630°C. At a measured temperature of 550°C the formation of the Mg_5Gd intermetallic phase and the peaks of crystalline Mg can be detected. As from 550°C the cooling advances no additional peaks appear on the line profiles. In the case of Mg4Y3Nd the solidification also starts with the initiation and growth of the α-Mg dendrites at a measured temperature of 625 °C. As the cooling advances the dendrites are followed by the Nd containing intermetallic phases. The binary $Mg_{12}Nd$ and the ternary $Mg_{14}Y_4Nd$ phases are first observed at 545 °C. Finally, solidification of $Mg_{24}Y_5$ can be observed at 320 °C.

Discussion

The Mg-Gd binary phase diagram is shown in Figure 6.

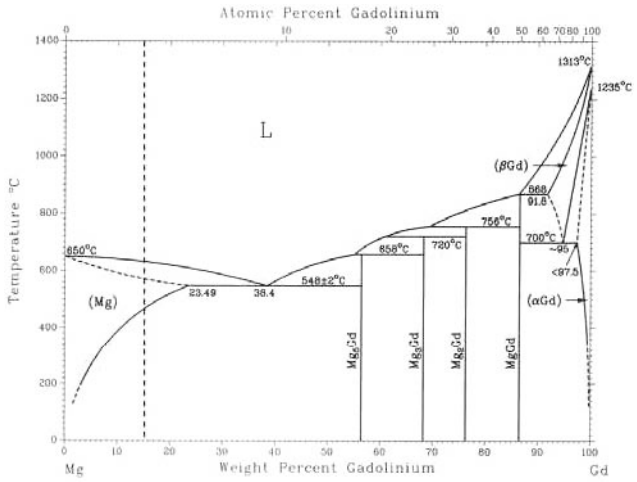

Figure 6. Mg-Gd binary phase diagram [3].

Comparing the phase diagram of Mg-Gd with the results from the *in situ* solidification tests, it can be seen that the experimental results correlate with the thermodynamic data from the literature. During cooling the system reaches its liquidus temperature at 627 °C and the formation of α-Mg grains start. On the diffraction pattern they can be barely detected as they are not in a fixed position but moving in the melt. As the cooling proceeds and the grains grow, their detection becomes more feasible. After further cooling; the system reaches its eutectic temperature (548 °C) where the solidification of Mg_5Gd takes place.

The thermodynamic simulation of the solidification of Mg-Y-Nd system was carried out with the software Pandat 8.1. The resulting section of the ternary phase diagram at an Nd content of 3 wt% is shown in Figure 7. The vertical line corresponds to a Y content of 4 wt%. According to the thermodynamic database the α-Mg dendrites initiate at 639 °C. They are followed by the $Mg_{12}Nd$ phase at 538 °C, while the solidification ends with the $Mg_{24}Y_5$ phase at 316 °C. The formation of the ternary $Mg_{14}Y_4Nd$ phase is not predicted by the thermodynamic software.

The determination of the solidification sequence by *in situ* synchrotron diffraction has some limitations. A compromise must be made between the cooling rate and the acquisition time. The crystallographic orientation of the solidifying grains plays a vital role. As these grains float in the melt without fixed orientation their detection is difficult. It is likely that the α-Mg grains can be detected properly for the first time as the system reaches the dendrites coherency point, the temperature where a continuous dendrite skeleton is built up.

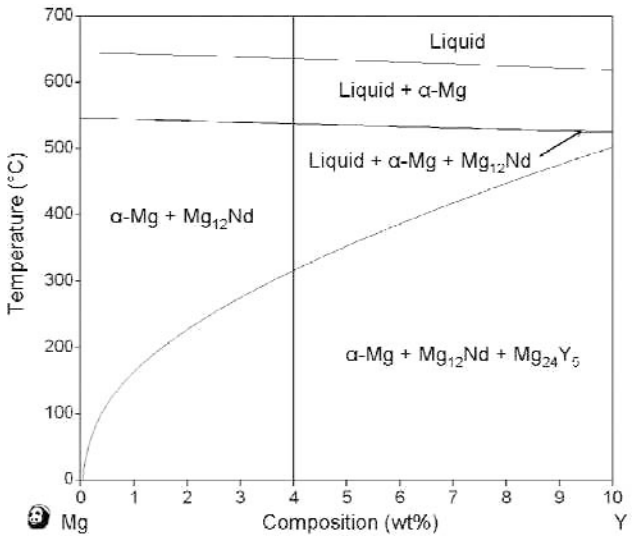

Figure 7 Section of the ternary Mg-Y-Nd phase diagram at a Nd content of 3 wt%, calculated by Pandat 8.1.

Despite these limitations, the onset temperatures, obtained experimentally by *in situ* diffraction and that predicted theoretically from the thermodynamic calculations, for the solidification of different phases correlate reasonably well. The ternary intermetallic phase $Mg_{14}Y_4Nd$ was only shown experimentally and not predicted by the thermodynamic simulations due to limited information available.

Conclusions

In situ solidification experiments were performed with a Bähr 805 A/D dilatometer, on Mg-15Gd and Mg-4Y-3Nd alloys by synchrotron diffraction, for the first time. From the results the following conclusions can be drawn:

- In the case of Mg-15Gd, first α-Mg solidifies at a measured temperature of 530 °C, followed by the solidification of α-Mg/Mg_5Gd at a measured temperature of 550 °C.
- In the case of Mg-4Y-3Nd the solidification starts with α-Mg which solidifies at a temperature of 625 °C followed by the solidification of the intermetallic particles; $Mg_{12}Nd$ and $Mg_{14}Y_4Nd$ at 545 °C and finally the $Mg_{24}Y_5$ phase at a temperature of 320 °C.

- The results for both of the alloys are in correlation with the data from thermodynamic databases. Furthermore *in situ* synchrotron diffraction reveals the presence of the ternary $Mg_{14}Y_4Nd$ phase and the onset of its solidification at 545 °C which could not be predicted by the simulations.

Acknowledgements

The authors would like to thank the Deutsches Elektronen-Synchrotron the provision of synchrotron radiation facilities in the framework of the proposal II-20100225.

References

[1] L.L. Rokhlin, *Magnesium Alloys Containing Rare Earth Metals, Structure and Properties*, Taylor & Francis, (2003).

[2] N. Hort et al., „Magnesium alloys as implant materials – Principles of property design for Mg–RE alloys" *Acta Biomaterialia* 6 (2010) 1714-1725.

[3] T.B. Massalski, *Binary Alloy Phase Diagrams,* ASM International Materials Park (1990).

[4] L.Y. Wei, G.L. Dunlop and H. Westengen, „Age hardening and precipitation in a cast magnesium - Rare-earth alloy" *Journal of Materials Science* 31 (1996) 387-397.

[5] G. Barucca et al., „Formation and evolution of the hardening precipitates in a Mg–Y–Nd alloy" *Acta Materialia* 59 (2011) 4151-4158.

[6] C. Antion et al., „Hardening precipitation in a Mg–4Y–3RE alloy" *Acta Materialia* 51(2003) 5335-5348.

[7] J.F. Nie and B.C. Muddle, „Characterisation of strengthening precipitate phases in a Mg–Y–Nd alloy" *Acta Materialia* 48 (2000) 1691-1703.

[8] P.J. Apps et al., „Phase compositions in magnesium-rare earth alloys containing yttrium, gadolinium or dysprosium" *Scripta Materialia* 48 (2003) 1023-1027.

[9] P.J. Apps et al., „Precipitation reactions in Magnesium-rare earth alloys containing Yttrium, Gadolinium or Dysprosium" *Scripta Materialia* 48 (2003) 475-479.

[10] H. Karimzadeh Ph.D Thesis Manchester University United Kingdom (1985).

[11] G. Requena et al., „The effect of the connectivity of rigid phases on strength of Al-Si alloys" *Advanced Engineering Materials* 13 (2011) 674-684.

[12] W.J. Boettinger et al., „Phase-field simulation of solidification *Annual Review of Materials Science,* 32 (2002) 163-194.

[13] Y. L. Liu, S and B. Kang, „The solidification process of AI-Mg-Si alloys *Journal of Materials Science* 32 (1997) 1443-1447.

[14] H. Jones, „Some effects of solidification kinetics on microstructure formation in aluminium-base alloys" *Materials Science and Engineering A* 413-414 (2005) 165-173.

[15] N. Iqba let al., „Nucleation kinetics during the solidification of aluminum alloys" *Journal of Non-Crystalline Solids* 353 (2007) 3640-3643.

[16] S.S. Babu et al., „Time-resolved X-ray diffraction investigation of primary weld solidification in Fe-C-Al-Mn steel welds" *Acta Materialia* 50 (2002) 4763-4781.

[17] O. Shuleshova et al., „*In situ* observations of solidification in Ti–Al–Ta alloys by synchrotron radiation" *Intermetallics* 19 (2011) 688-692.

[18] P. Staron et al., „In situ experiments with synchrotron high-energy X-rays and neutrons" *Advanced Engineering Materials* 13 (2011) 685-689.